International Journal of Engineering, Mathematical and Physical Sciences
ISSN: 2517-9934
Vol:8, No:5, 2014

MHD Stagnation Point Flow towards a Shrinking Sheet with Suction in an Upper-Convected Maxwell (UCM) Fluid

K. Jafar, R. Nazar, A. Ishak, I. Pop

***Abstract*—**The present analysis considers the steady stagnation point flow and heat transfer towards a permeable shrinking sheet in an upper-convected Maxwell (UCM) electrically conducting fluid, with a constant magnetic field applied in the transverse direction to flow and a local heat generation within the boundary layer, with a heat generation rate proportional to $(T-T_\infty)^p$. Using a similarity transformation, the governing system of partial differential equations is first transformed into a system of ordinary differential equations, which is then solved numerically using a finite-difference scheme known as the Keller-box method. Numerical results are obtained for the flow and thermal fields for various values of the stretching/shrinking parameter λ, the magnetic parameter M, the elastic parameter K, the Prandtl number Pr, the suction parameter s, the heat generation parameter Q, and the exponent p. The results indicate the existence of dual solutions for the shrinking sheet up to a critical value λ_c whose value depends on the value of M, K, and s. In the presence of internal heat absorption $(Q<0)$, the surface heat transfer rate decreases with increasing p but increases with parameters Q and s, when the sheet is either stretched or shrunk.

***Keywords*—**Magnetohydrodynamic (MHD), boundary layer flow, UCM fluid, stagnation point, shrinking sheet.

I. Introduction

THE study of flow and heat transfer near a stagnation point, where fluids flow impinging normally or obliquely to plane surfaces, has applications in many practical situations. Theories on the stagnation flow and associated heat transfer characteristics have been used to enhance many technological developments. Since the development of an exact solution for the two dimensional stagnation flow by Hiemenz [1] and an exact similar solution for the corresponding thermal field by Eckert [2], studies on the flow and heat transfer near a stagnation point has produced extensive theoretical and numerical results for stagnation point flow and heat transfer. Stagnation point flow and related heat transfer problems are also encountered in problems involving stretching or shrinking sheets. Some recent examples of these studies can be found in the works of Ishak et al. [3], [4], Hayat et al. [5], and Jafar et al. [6]. All previous studies on the flow over a shrinking surface such as that by Miklavčič and Wang [7], and Wang [8], [9], reported some interesting differences in the flow and heat transfer characteristics of a shrinking sheet as compared to a stretching sheet, specifically in the existence and non-uniqueness of solutions.

In the studies on convective heat transfer, the flow is usually driven by either a natural or a mixed convection. Alternatively, a convective flow may also develop due to internal heat generation or absorption within the flow. Mealey and Merkin [10] studied the natural convection boundary layer flow on a vertical surface with heat generated within the boundary layer, by assuming a local heat generation rate proportional to $(T-T_\infty)^p$ where T is the local temperature, T_∞ is the ambient temperature and $p \geq 1$, a constant. They found that for $2 < p < 4$, the local heating has significant effect. Using the same assumption on the rate of heat generation, Merkin [11] considered a similar study, with a further assumption of a thermally insulated surface. It was found that the development of the flow from the leading edge depend critically on the exponent p, with singularity developing in the boundary layer solutions for $2 < p < 5$. More recent studies on convective flow with internal heat generation can be found in the work of Merkin and Pop [12] and Merkin [13].

The objective of the present paper is to investigate the stagnation point flow and heat transfer over a permeable stretching/shrinking sheet in an upper convected Maxwell fluid (UCM), with an externally applied magnetic field, in the presence of wall suction and internal heat generation/absorption. The same form of heat generation rate used by Mealey and Merkin [10] is assumed. The upper convected Maxwell (UCM) fluid model is favored by many researchers to represent the viscoelastic fluid, which is an important class of non-Newtonian fluid encountered in many engineering and industrial processes today. Recent studies on the stagnation point flow of a UCM fluid was done by Sadeghy et al. [14], Kumari and Nath [15], Hayat et al. [16] and Jafar et al. [17]. The present paper will include both the stretching and shrinking sheets, and will include the effects of the exponent of the heat generation rate, on the flow and heat transfer characteristics.

K. Jafar is with the Faculty of Engineering & Built Environment, Universiti Kebangsaan Malaysia, 43600 UKM Bangi, Selangor, Malaysia (phone: 603-89216962; fax: 603-89216960; e-mail: kjafar61@ gmail.com).

R. Nazar and A. Ishak are with School of Mathematical Sciences, Faculty of Science & Technology, Universiti Kebangsaan Malaysia, 43600 UKM Bangi, Selangor, Malaysia (e-mail: rmn72my@yahoo.com, anuarishak001@yahoo.com).

I. Pop is with the Department of Mathematics, Babeş-Bolyai University, R-400084 Cluj-Napoca, Romania(e-mail: popm.ioan@yahoo.co.uk).

II. Mathematical Formulation

Consider a steady stagnation point flow towards a permeable stretching/shrinking sheet in an upper-convected Maxwell (UCM) electrically conducting fluid. It is assumed that the velocity of the shrinking sheet is $u_w(x) = c\,x$, while the flow velocity outside the boundary layer(inviscid fluid) is $u_e(x) = a\,x$, where $a\,(>0)$ and c are constants, with $c>0$ for a stretching sheet, and $c<0$ for a shrinking sheet. It is also assumed that the constant mass transfer velocity is v_w, with $v_w<0$ for suction and $v_w>0$ for injection (withdrawal). Further, it is assumed that the uniform temperature of the sheet is T_w, whereas that of the ambient fluid is T_∞. The fluid is bounded by the stretching/shrinking sheet at $y=0$ and the flow occupies the space $y>0$. A constant magnetic field of strength B_0 is applied in the transverse direction to flow. The electric and induced magnetic fields are negligible. Following Merkin [11] and Hayat et al. [16], the basic equations for the problem under consideration which, on applying the boundary layer approximations can be written as

$$\frac{\partial u}{\partial x}+\frac{\partial v}{\partial y}=0, \tag{1}$$

$$u\frac{\partial u}{\partial x}+v\frac{\partial u}{\partial y}=u_e\frac{du_e}{dx}+\nu\frac{\partial^2 u}{\partial y^2}- k_0\left(u^2\frac{\partial^2 u}{\partial x^2}+v^2\frac{\partial^2 u}{\partial y^2}+2uv\frac{\partial^2 u}{\partial x\partial y}\right)-\frac{\sigma B_0^2}{\rho}\left(u-u_e+k_0 v\frac{\partial u}{\partial y}\right), \tag{2}$$

$$u\frac{\partial T}{\partial x}+v\frac{\partial T}{\partial y}=\alpha\frac{\partial^2 T}{\partial y^2}+\frac{Q_0}{\rho C_p}(T-T_\infty)^p, \tag{3}$$

with the boundary conditions,

$$\begin{aligned} &u=u_w(x),\quad v=v_w,\quad T=T_w \quad \text{at} \quad y=0\\ &u\to u_e(x),\quad T\to T_\infty \quad \text{as} \quad y\to\infty, \end{aligned} \tag{4}$$

where u and v are the velocity components along the $x-$ and $y-$ axes, respectively, ν is the kinematic viscosity, k_0 is the elastic parameter of the UCM fluid, α is the thermal diffusivity, ρ is the density, σ is the electrical conductivity and C_p is the specific heat at a constant pressure.The term $Q_0(T-T_\infty)^p$, where p is a constant, assumed to be the amount of heat generated or absorbed per unit volume, for which Q_0 may take on either positive or negatives values. If $Q_0>0$, then it represents heat generation and on the other hand when $Q_0<0$, it represents heat absorption.

In order to solve (1)–(3) with the boundary conditions (4), we consider the following similarity variables:

$$\psi=(\nu a)^{1/2}xf(\eta),\quad \eta=(a/\nu)^{1/2}y,\quad \theta(\eta)=(T-T_\infty)/(T_w-T_\infty), \tag{5}$$

where ψ is the stream function defined as $u=\partial\psi/\partial y$, and $v=-\partial\psi/\partial x$, which identically satisfies (1). Substituting (5) into (2) and (3), we obtain the following nonlinear ordinary differential equations

$$f'''+f\,f''+1-f'^2+K\left(f^2f'''-2f\,f'\,f''\right)-M\left(f'-1-K\,f\,f''\right)=0 \tag{6}$$

$$\frac{1}{\Pr}\theta''+f\theta'+Q\theta^p=0, \tag{7}$$

where primes denote differentiation with respect to η. The boundary conditions (4) now become

$$\begin{aligned} &f(0)=s,\quad f'(0)=c/a=\lambda,\quad \theta(0)=1\\ &f'(\eta)\to 1,\quad \theta(\eta)\to 0 \quad \text{as} \quad \eta\to\infty. \end{aligned} \tag{8}$$

Here $K=ak_0\,(\geq 0)$ is the dimensionless elastic parameter also known as Deborah or Weissenger number, $\Pr=\nu/\alpha$ is the Prandtl number, λ is the stretching $(\lambda>0)$ or shrinking $(\lambda<0)$ parameter, $s=-v_w/(a\nu)^{1/2}$ is the mass transfer parameter with $s>0$ for suction and $s<0$ for injection, and $Q=Q_0(T_w-T_\infty)/(a\rho C_p)$ is the dimensionless heat generation $(Q>0)$ or absorption $(Q<0)$ coefficient. We notice that for $K=s=\lambda=M=0$, (6) reduces to the classical Hiemenz [1] problem.

The quantities of physical interest in this problem are the skin friction coefficient C_f, and the local Nusselt number Nu_x, which are defined as

$$C_f=\frac{\tau_w}{\rho u_e^2(x)},\quad Nu_x=\frac{x\,q_w}{k(T_w-T_\infty)}, \tag{9}$$

where τ_w is the wall shear stress,and q_w is the surface heat flux and are given by

$$\tau_w=\mu(1+K)\left(\frac{\partial u}{\partial y}\right)_{y=0},\quad q_w=-k\left(\frac{\partial T}{\partial}\right)_{y=0}, \tag{10}$$

where μ is the dynamic viscosity. Substituting (5) into (10) and using (9), we get

$$\mathrm{Re}_x^{1/2}C_f=(1+K)f''(0),\quad \mathrm{Re}_x^{1/2}Nu_x=-\theta'(0), \tag{11}$$

where $\mathrm{Re}_x^{1/2}=u_e(x)x/\nu$ is the local Reynolds number.

III. Results and Discussion

The nonlinear ordinary differential equations (6) and (7) subject to the boundary conditions (8) have been solved numerically using the Keller-box method. The velocity $f'(\eta)$

and temperature $\theta(\eta)$ profiles are obtained for various values of the governing parameters, namely the magnetic parameter M, the elastic parameter K, the stretching/shrinking parameter λ, the Prandtl number Pr, the mass transfer parameter s, the heat generation parameter Q, and exponent p of the heat generation term. The values of the skin friction coefficient $(1+K)f''(0)$ and the local Nusselt number $-\theta'(0)$ for various values of the governing parameters are also computed to investigate the effects of these parameters on the surface shear stress and the surface heat transfer. In order to assess the accuracy of the numerical method used, we have compared some of our results on the flow for the non-magnetic case for a non-permeable surface $(M = s = \lambda = 0)$, with those obtained in an earlier work on UCM fluid, Jafar et al. [17]. The values of the surface velocity gradient $f''(0)$ obtained are found to be in very good agreement. We have also compared the values of $f''(0)$ and $-\theta'(0)$ obtained to those computed using a shooting method, and found good agreement. Therefore, the developed code can be used with confidence. For the present study we will focus on the case of heat absorption, that is the case $Q < 0$. The main reason for this restriction is because the results for the case $Q < 0$ are more consistent and show better convergence. Since (6) and (7) are uncoupled, the flow field is not affected by the thermal field, thus the Prandtl number, the heat absorption parameter Q and the exponent p has no influence on the skin friction coefficient and the velocity profiles.

Table I presents values of the skin friction coefficient $(1+K)f''(0)$ and the local Nusselt number $-\theta'(0)$ for various values of the magnetic parameter M, the elastic parameter K, and the parameter λ (for both the stretching and shrinking sheets), when the other parameters are fixed at $\text{Pr} = 1, s = 2, p = 4,$ and $Q = -2$. As seen from Table I, both the skin friction coefficient $(1+K)f''(0)$ and the local Nusselt number $-\theta'(0)$ increase with the increase of the magnetic parameter M but decrease with increasing values of the elastic parameter K. However the increase/decrease in the local Nusselt number is small compared to that of the skin friction coefficient. This trend holds for both the stretching and shrinking sheets.

Figs. 1 to 5 present the variations of the velocity profiles $f'(\eta)$ with the magnetic parameter M, the stretching parameter λ, the elastic parameter K, and the mass transfer parameter s (for the shrinking and stretching sheets), respectively. Figs. 6-10 present the variations of the temperature profiles $\theta(\eta)$ with the stretching parameter λ, the Prandtl number Pr, the exponent p, the heat generation parameter Q, and the mass transfer parameter s, respectively. All the sample profiles satisfy the far field boundary conditions (8) asymptotically, thus supporting the numerical results obtained. From Figs. 1 and 2, we see that increasing the value of M and λ result in a decrease in the boundary layer thickness and an increase in the fluid velocity $f'(\eta)$ and the velocity gradient at the wall $f''(0)$, whereas Fig. 3 indicates the opposite trend for the elastic parameter K. Figs. 4 and 5 show that for both the shrinking and stretching sheets, the velocity profiles $f'(\eta)$ and the velocity gradient at the wall $f''(0)$ increase with s for $s < 0$, but decrease for $s > 0$. Since $s < 0$ signifies injection at the wall and $s > 0$ signifies suction at the wall, an increase in either suction or injection will result in a decrease in the fluid velocity and the skin friction coefficient.

TABLE I
VALUES OF $f''(0)$ AND $-\theta'(0)$ FOR VARIOUS VALUES OF M AND K WHEN $\text{Pr} = 1, s = 2, p = 4$ AND $Q = -2$

M	$(1+K)f''(0)$				$-\theta'(0)$			
	$\lambda = 0.5$		$\lambda = -0.5$		$\lambda = 0.5$		$\lambda = -0.5$	
	$K = 0.1$	$K = 0.2$	$K = 0.1$	$K = 0.2$	$K = 0.1$	$K = 0.2$	$K = 0.1$	$K = 0.2$
0	1.0292	0.8253	3.0176	2.6238	2.4750	2.4638	2.2911	2.2606
0.5	1.1303	0.9466	3.3510	3.0230	2.4782	2.4682	2.3030	2.2769
1	1.2244	1.0596	3.6553	3.3870	2.4809	2.4720	2.3129	2.2902
1.5	1.3131	1.1667	3.9384	3.7270	2.4834	2.4753	2.3215	2.3014
2	1.3975	1.2692	4.2053	4.0493	2.4856	2.4783	2.3291	2.3112

TABLE II
CRITICAL VALUES λ_c AND CORRESPONDING VALUES OF $f''(0)$ AND $-\theta'(0)$ FOR DIFFERENT VALUES OF M WHEN $\text{Pr} = 1, K = 0.2, p = 4$ AND $Q = -2$

M	λ_c		$(1+K)f''(0)$		$-\theta'(0)$	
0.5	$s = 1$	$s = 2$	$s = 1$	$s = 2$	$s = 1$	$s = 2$
	-2.37038	-3.821	3.3161	7.8181	1.0485	1.4001
1	-2.75518	-4.40327	4.3081	10.3505	1.0152	1.3432

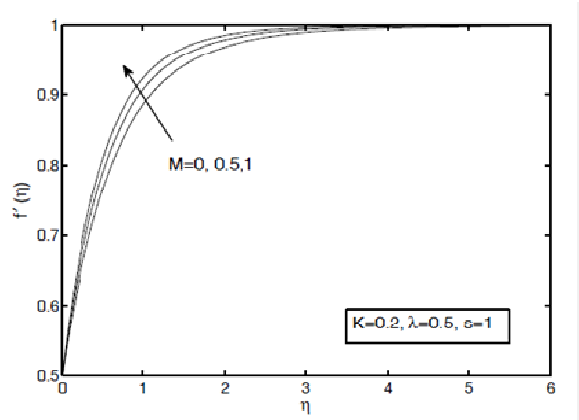

Fig. 1 Velocity profiles $f'(\eta)$ for various values of the magnetic parameter M when $K = 0, \lambda = 0.5, \Pr = 1, s = 1, p = 4$, and $Q = -2$

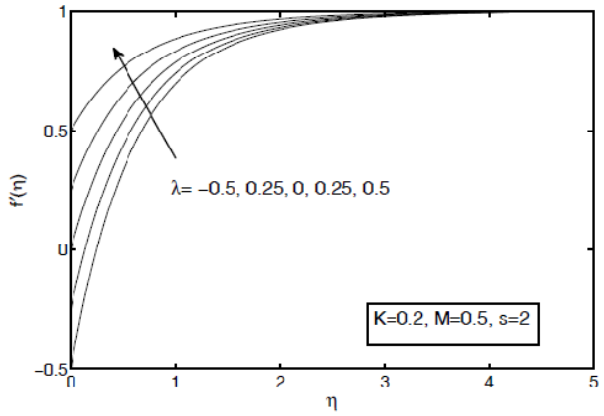

Fig. 2 Velocity profiles $f'(\eta)$, for various values of the stretching parameter λ, when $M = 0.5, K = 0.2$, and $s = 2$

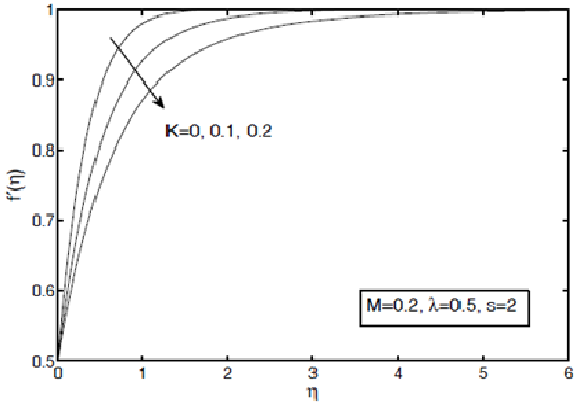

Fig. 3 Velocity profiles $f'(\eta)$, for various values of the elastic parameter K, when $M = 0.2, \lambda = 0.5$, and $s = 2$

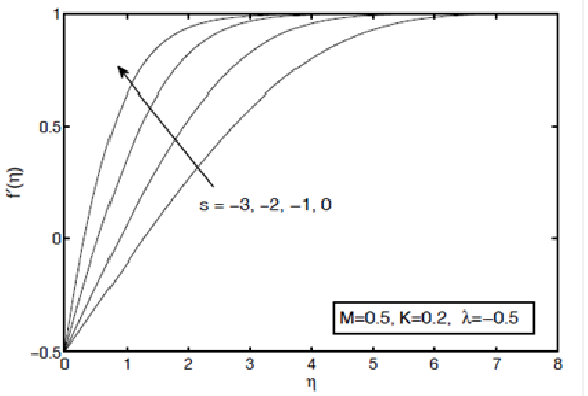

Fig. 4 Velocity profiles $f'(\eta)$, for various values of the mass transfer parameter $s < 0$, for the shrinking sheet with $\lambda = -0.5$, when $M = 0.5$, and $K = 0.2$

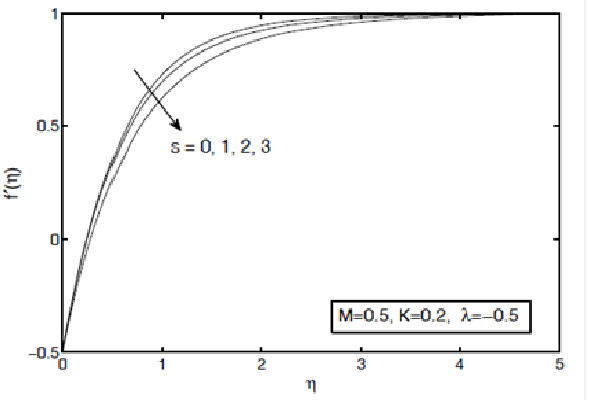

Fig. 5 Velocity profiles $f'(\eta)$, for various values of the mass transfer parameter $s > 0$, for the shrinking sheet with $\lambda = -0.5$, when $M = 0.5$, and $K = 0.2$

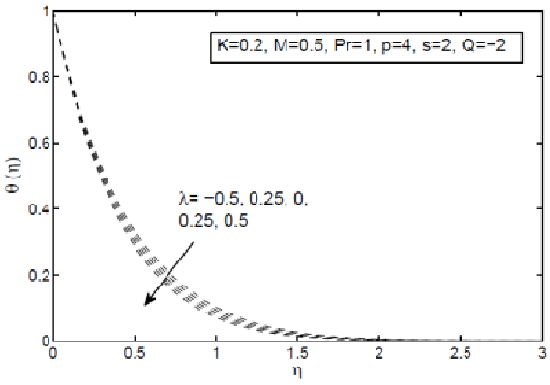

Fig. 6 Temperature profiles $\theta(\eta)$, for various values of the stretching parameter λ, when $M = 0.5, K = 0.2, \Pr = 1, p = 4, s = 2$, and $Q = -2$

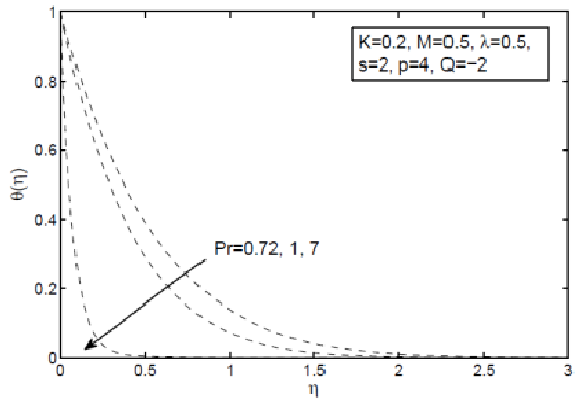

Fig. 7 Temperature profiles $\theta(\eta)$, for various values of the Prandtl number Pr, when $M = 0.5, K = 0.2, \lambda = 0.5, p = 4, s = 2$, and $Q = -2$

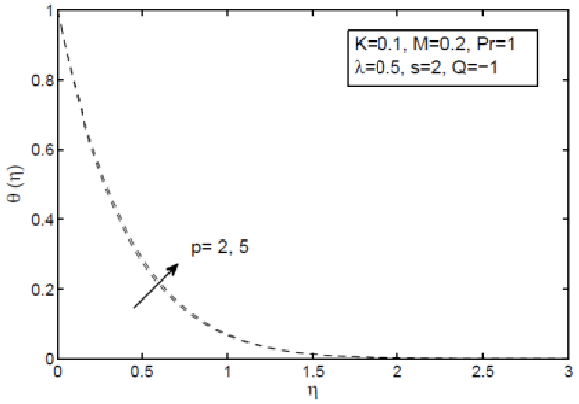

Fig. 8 Temperature profiles $\theta(\eta)$, for various values of the exponent p, when $M = 0.5, K = 0.1, \Pr = 1, \lambda = 0.5, s = 2$, and $Q = -1$

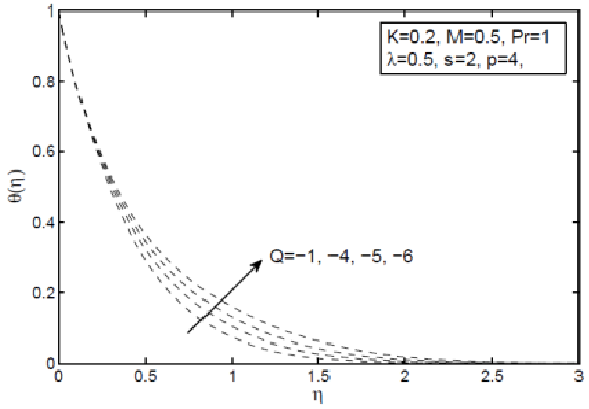

Fig. 9 Temperature profiles $\theta(\eta)$, for various values of the heat generation parameter Q, when $M = 0.5, K = 0.1, \Pr = 1,$ $\lambda = 0.5, s = 2,$ and $p = 4$

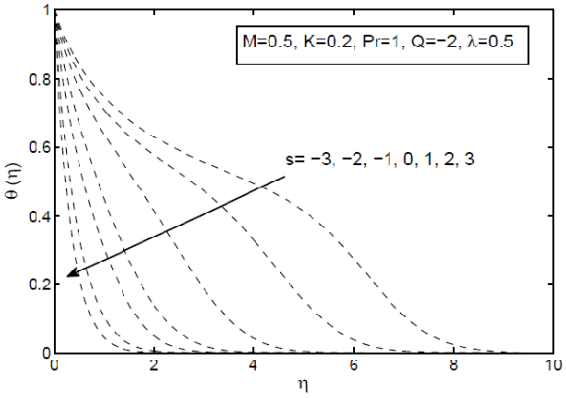

Fig. 10 Temperature profiles $\theta(\eta)$, for various values of the mass transfer parameter s, forthe stretching $(\lambda = 0.5)$ sheetwhen $M = 0.5, K = 0.2, \Pr = 1, Q = -2$

Figs. 6-10 show that the temperature profiles $\theta(\eta)$, increase with the parameters p but decreases with the increasing values of $\lambda, \Pr,$ and s. Furthermore, as the value of $\lambda, \Pr,$ and s increases, the thermal boundary layer thickness decreases. This implies that the local Nusselt number $-\theta'(0)$ increases with $\lambda, \Pr$ and s. Our computations indicate that the local Nusselt number $-\theta'(0)$ decreases with the increase in p but increases with $|Q|$. Thus increasing the exponent p will decrease the surface heat transfer rate, while increasing the magnitude of the heat absorption coefficient $|Q|$ increases the surface heat transfer rate. Fig. 6 indicates that increase stretching will also increase the local Nusselt number $-\theta'(0)$, hence enhancing the heat transfer rate at the surface, while increase shrinking reduces it. On the other hand, Fig. 10 shows that, for both shrinking and stretching sheets, increasing the magnitude of the mass transfer parameter $|s|$ will decrease the thermal boundary layer thickness and increase thelocal Nusselt number $-\theta'(0)$ for $s > 0$, whereas for $s < 0$, increasing $|s|$ thickens the boundary layer and decreases thelocal Nusselt number $-\theta'(0)$. Thus in general, suction enhances the heat transfer rate at the surface while injection reduces it.

TABLE III
CRITICAL VALUES λ_c AND CORRESPONDING VALUES OF $f''(0)$ AND $-\theta'(0)$ FOR DIFFERENT VALUES OF K WHEN $s = 2, M = 0.5, p = 4$ AND $Q = -2$

K	λ_c	$(1+K) f''(0)$	$-\theta'(0)$
0.1	-3.6013	5.8907	1.4318
0.2	-3.821	7.8181	1.4001

Figs. 11-13 present the variations of the skin friction coefficient $(1+K) f''(0)$, with λ for various values of the magnetic parameter M, the mass transfer parameter s, and

the elastic parameter K. In the case of the stretching sheet $(\lambda > 0)$, the figures show that for all values of the $M, K,$ and λ considered, the magnitude of the skin friction coefficient $\left|(1+K) f''(0)\right|$ decreases when $0 < \lambda < 1$, is zero at $\lambda = 1$, and increases when $\lambda > 1$. Furthermore, $\left|(1+K) f''(0)\right|$ also increases with the magnetic parameter M, but decreases slightly with K and s for all values of the stretching parameter λ. For the case of the shrinking sheet $(\lambda < 0)$, we found that dual solutions exist and there is a minimum value λ_c of the shrinking parameter for which solution exists, and its magnitude $|\lambda_c|$ increases as the value of $M, K,$ and s increases. At $\lambda = \lambda_c$, the solution is unique, while dual solutions exist for some range of $\lambda_c < \lambda < 0$. The critical values λ_c and the corresponding values of the skin friction coefficient $(1+K) f''(0)$, and the local Nusselt number $-\theta'(0)$ for different values of the magnetic parameter M and K are given in Tables II and III. As seen from the tables, the value of $|\lambda_c|$ and the corresponding value of $(1+K) f''(0)$, increase with the parameters $M, K,$ and s. Thus the presence of suction, magnetic field and fluid elasticity expands the solution domain. However these three parameters differ in terms of their effects on the wall shear stress. It is observed that, for both the stretching and shrinking sheets, the magnetic field increases the wall shear stress. In contrast, the presence of suction and fluid elasticity reduces the wall shear stress, as indicated by the decrease in the values of the skin friction coefficient as the values of s and K increase. The results observed on the flow characteristics agree with most earlier studies on the effect of magnetic field on the momentum transfer over a flat plate. For the shrinking sheet, the value of the skin friction coefficient initially decreases with s and K, but the trend changes when the shrinking magnitude becomes larger. Thus for large shrinking magnitude, both the suction and the fluid elasticity increase the wall shear stress.

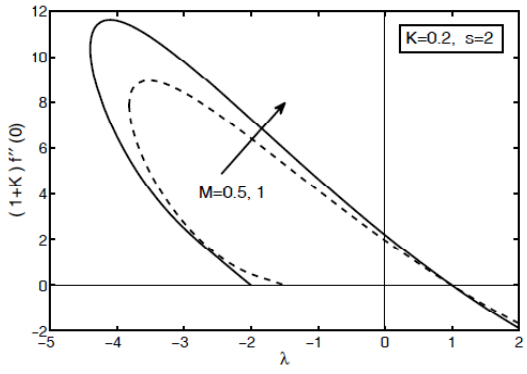

Fig. 11 Variations of the skin friction coefficient $(1+K) f''(0)$ as a function of λ, with the magnetic parameter M, when $K = 0.2, p = 4,$ and $s = 2$

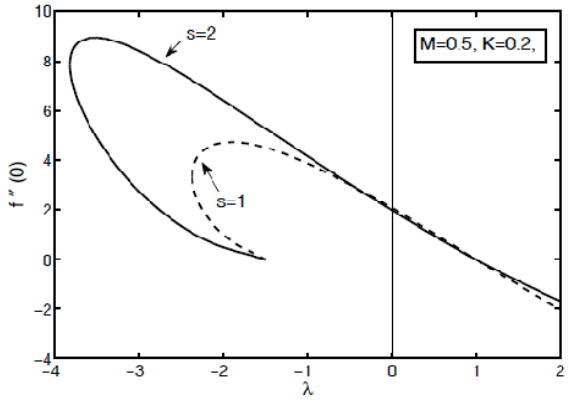

Fig. 12 Variations of the skin friction coefficient $(1+K) f''(0)$ as a function of λ, with the mass transfer parameter s, when $K = 0.2,$ and $M = 0.5$

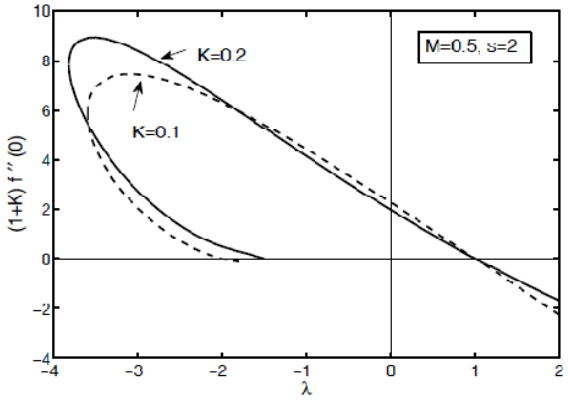

Fig. 13 Variations of the skin friction coefficient $(1+K) f''(0)$ as a function of λ, with the elastic parameter K, when $K = 0.2, M = 0.5,$ and $s = 2$

Figs. 14 to 17 show the variations of the heat transfer rate at the surface, represented by the local Nusselt number $-\theta'(0)$ (as a function of λ) with the heat generation parameter Q, the mass transfer parameter s, the exponent p, and the elastic parameter K, respectively. As seen from these figures, the values of $-\theta'(0)$ increases for the stretching sheet $(\lambda > 0)$ but decreases for the shrinking sheet $(\lambda < 0)$ for both the first and second branch of solutions. Figs. 14 to 16 indicate that $-\theta'(0)$ decreases with increasing p but increases with parameters Q and s, for both the stretching and shrinking sheets. The trend is the same for both the first and second branch of solutions. In Fig. 17, $-\theta'(0)$ shows very little variations with M when the sheet is stretched, but when the sheet is shrunk, the first branch of solutions increases quite significantly with M. In comparison, the variations of $-\theta'(0)$ with the elastic parameter K show a more complicated

pattern, as seen in Fig. 18. For the stretching sheet, the values of $-\theta'(0)$ decreases as K increases when $0 \le \lambda < 1$, but increases with K when $\lambda \ge 1$. A similar pattern is observed in the first branch of solution for the shrinking sheet, with the values of $-\theta'(0)$ initially decreasing as K increases, and eventually changing to the opposite trend as the shrinking magnitude gets closer to the critical value λ_c. For the second branch of solutions, $-\theta'(0)$ increases with K. Therefore, increasing the heat absorption, suction at the wall and the Prandtl number will result in a thinning of the thermal boundary layer and enhance the surface heat transfer rate, while increasing the exponent p reduces the surface heat transfer rate. The magnetic field enhances the surface heat transfer rate of the shrinking sheet but has very little effect on stretching sheet. When the stretching velocity of the sheet is less than the free stream velocity, the fluid elasticity slightly decreases the surface heat transfer rate. When the stretching velocity exceeds the free stream velocity, the effect of the fluid elasticity is reversed.

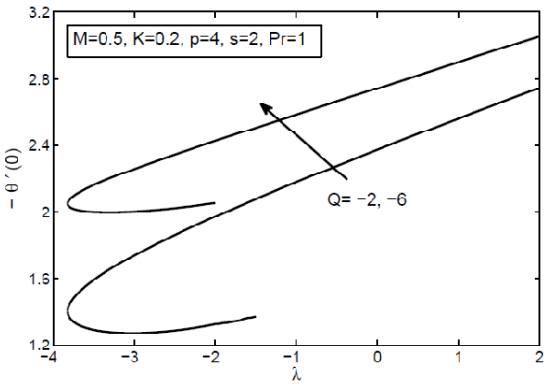

Fig. 14 Variations of the local Nusselt number $-\theta'(0)$ as a function of λ, with the heat generation parameter Q, when $K = 0.2, M = 0.5, p = 4,$ and $s = 2$

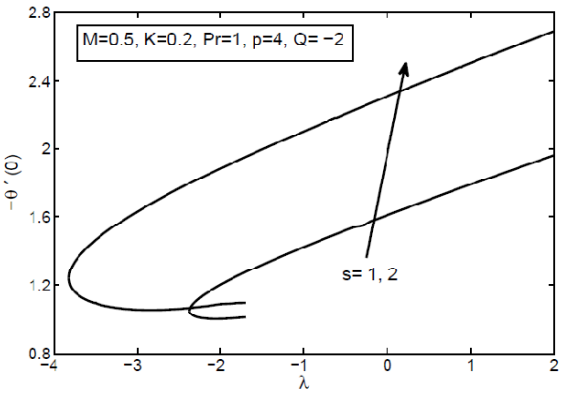

Fig. 15 Variations of the local Nusselt number $-\theta'(0)$ as a function of λ, with the mass transfer parameter s, when $K = 0.2, M = 0.5, p = 4,$ and $Q = -2$

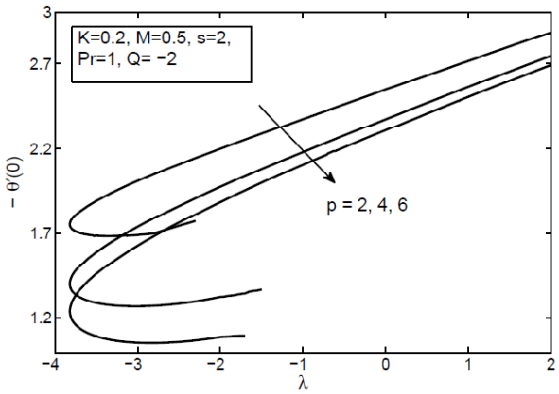

Fig. 16Variations of the local Nusselt number $-\theta'(0)$ as a function of λ, with the exponent p, when $K = 0.2, M = 0.5, p = 4,$ and $Q = -2$

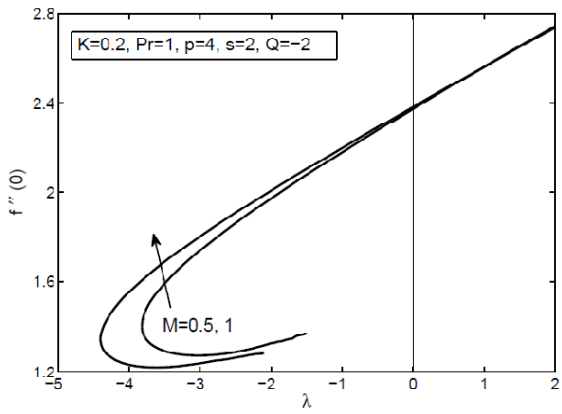

Fig. 17 Variations of the local Nusselt number $-\theta'(0)$ as a function of λ, with the magnetic parameter M, when $K = 0.2, s = 2, p = 4,$ and $Q = -2$

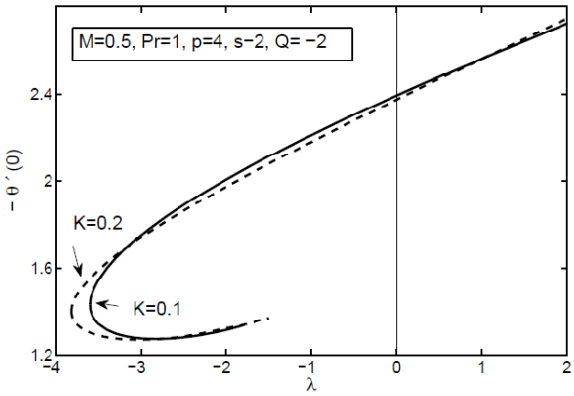

Fig. 18 Variations of the local Nusselt number $-\theta'(0)$ as a function of λ, with the elastic parameter K, when $M = 0.5, s = 2, p = 4,$ and $Q = -2$

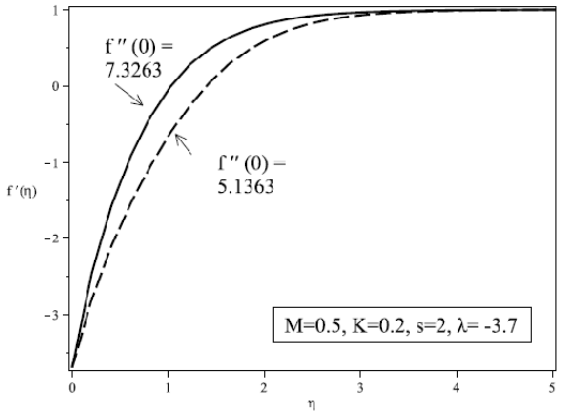

Fig. 19 Velocity profiles $f'(\eta)$ for the first solution (full line) and second solution (dotted lines) solution when $M = 0.5, s = 2, p = 4,$ and $\lambda = -3.7$

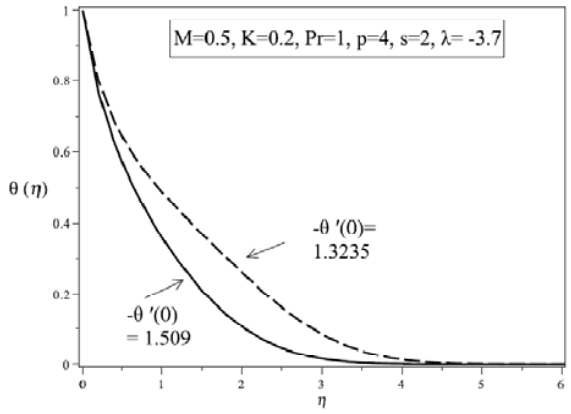

Fig. 20 Temperature profiles $\theta(\eta)$ for the first solution (full line) and second solution (dotted lines) solution when $M = 0.5, s = 2, p = 4,$ and $\lambda = -3.7$

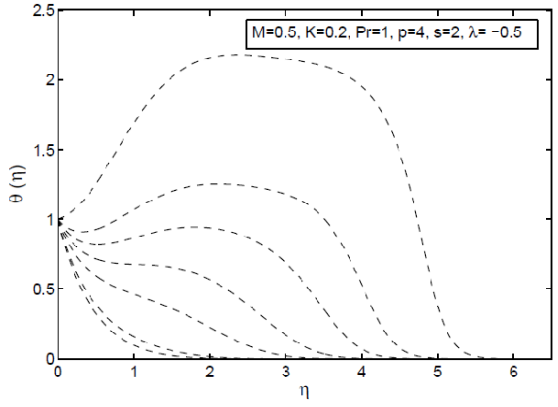

Fig. 21 Temperature profiles $\theta(\eta)$, supporting the existence of multiple solutions of the energy equation when $M = 0.5, K = 0.2, s = 2, p = 4,$ and $\lambda = -0.5$

Figs. 19-20 present the velocity $f'(\eta)$ and temperature $\theta(\eta)$ profiles supporting the existence of dual solutions when $M = 0.5, K = 0.2,\ p = 4, s = 2, \Pr = 1$ and $\lambda = -0.82$. We mention here that, in the case of the shrinking sheet, multiple solutions for the temperature profiles can be found for each velocity profile obtained. Fig. 21 gives samples of such solution when $M = 0.5, K = 0.2, p = 4, s = 2, \Pr = 1$ and $\lambda = -0.5$.

IV. Conclusion

In this paper, we have considered similarity solutions for the steady stagnation flow and heat transfer towards a permeable shrinking sheet in an upper-convected Maxwell (UCM) electrically conducting fluid, with a constant magnetic field applied in the transverse direction to flow and a local heat generation within the boundary layer. We investigated the effects of the stretching parameter λ, the magnetic parameter M, the elastic parameter K, the Prandtl number $\Pr$, the mass transfer parameter s, the heat generation coefficient Q, and the exponent p of the heat generation term in the energy equation, on the flow and heat transfer characteristics. For the present study, the Prandtl number is fixed at $\Pr = 1$ and the analysis is focused on the case of wall suction and heat absorption. It is found that the solution for the stretching sheet exists and is unique for all values of the stretching parameter λ while solutions for the shrinking sheet only exist when the magnitude of the stretching parameter is less than $|\lambda_c|$ for some limiting value λ_c, with dual solutions found for some ranges of λ. It was shown that the solution is unique for $\lambda \geq 0$, and dual solutions are found for some $\lambda > \lambda_c$ of the shrinking parameter. Furthermore, it is found that the increasing the magnetic parameter M, the elastic parameter K, and the suction parameter s expands the solution domain. For both the stretching and shrinking sheets, the magnetic field increases the wall shear stress, for large shrinking magnitude, both the suction and the fluid elasticity also increase the wall shear stress. However for the stretching sheet, the wall suction and fluid elasticity reduces the wall shear stress. In the presence of internal heat absorption $(Q < 0)$, the surface heat transfer rate decreases with increasing p but increases with parameters Q and s, when the sheet is either stretched or shrunk. Increasing the magnetic parameter has little effect on the surface heat transfer when the sheet is stretched, however for the shrinking sheet, it causes a significant increase in the surface heat transfer rate. When the sheet is stretched with a velocity less than the free stream velocity, the surface heat transfer rate slightly decreases as the fluid elasticity increases, and vice-versa.

ACKNOWLEDGMENT

The authors gratefully acknowledged the financial support received in the form of a GGPM research grant from the Universiti Kebangsaan Malaysia.

REFERENCES

[1] K. Hiemenz,"Dei grenzschicht an einem in den gleichformigen Flussigkeitsstrom eingetauchten geraden,"*Kreiszylinder. Dingl. Polytech. J.*,vol. 32, pp. 321–410, 1911.

[2] E. R. G. Eckert, "Die berechnung des warmeuberganges in der laminaren grenzschicht umstromter korper,"*VDI Forschungsheft* Vol. 416, pp. 1–23, 1942.

[3] A. Ishak, K. Jafar, R.Nazar, and I. Pop,"MHD stagnation point flow towards a stretching sheet,"*Physica A* Vol. 388, pp. 3377–3383, 2009.

[4] A. Ishak, Y. Y. Lok, I. Pop,"Stagnation-point flow over a shrinking sheet in a micropolar fluid," *Chem. Eng. Comm*., Vol. 197,pp. 1417–1427, 2010

[5] T. Hayat, Z. Abbas, M. Sajid,"MHD stagnation-point flow of an upper convected-Maxwell fluid over a stretching surface,"*Chaos Soliton Fractals*, Vol. 39, pp. 840–848, 2009.

[6] K. Jafar, R. Nazar, A. Ishak, and I. Pop,"MHD flow and heat transfer over stretching/shrinking sheets with external magnetic field, viscous dissipation and Joule effects," *Can. J. Chem. Eng*., Vol. 90, No. 5, pp. 1336–1346, 2012.

[7] M. Miklavčič, and C. Y. Wang,"Viscous flow due to a shrinking sheet," *Quart. Appl. Math.,* Vol. 64,pp. 283–290, 2006.

[8] C. Y. Wang,"Liquid film on an unsteady stretching sheet," *Quart. Appl. Math*., Vol, 48,pp. 601–610, 1990.

[9] C. Y. Wang,"Stagnation flow towards a shrinking sheet,"*Int. J. Non-Linear Mech*., Vol. 43, pp. 377–382, 2008.

[10] L. Mealey, and J. H. Merkin,"Free convection boundary layers on a vertical surface in a heat generating porous medium,"*IMA J. Appl. Math.*, Vol.73, pp. 231–253, 2008.

[11] H. Merkin, "Natural convective boundary-layer flow in a heat generating porous medium with a prescribed wall heat flux," *J. Appl. Math. Phys. (ZAMP)*, Vol. 60, pp. 543–564, 2009.

[12] H. Merkin, and I. Pop,"Natural convection boundary-layerflow in a porous medium with temperature-dependent boundary conditions," *Transp. Porous Med*., Vol. 85,pp. 397–414, 2010.

[13] H. Merkin,"Free convection boundary layers on a vertical suface in a heat generating porous medium: Similarity solutions,"*Quart. J. Mech Applied Math*., Vol. 61, No. 2, pp.205–218, 2008.

[14] Sadeghy K, Hajibeygi H, Taghavi SM (2006) Stagnation-point flow of upper-convected Maxwell fluid. Int. J. Non-Linear Mech. 41: 1242–1247.

[15] M. Kumari, and G. Nath,"Steady mxed convection stagnation-point flow of upper-convected Maxwell fluids with magnetic field,"*Int. J. Non-Linear Mech.*, Vol. 44, pp. 1048–1055, 2009.

[16] T. Hayat, M. Awais, M. Qasim, and A.Hendi,"Effects of mass transfer on the stagnation point flow of an upper-convected Maxwell (UCM) fluid,"*Int. J. Heat Mass Transfer*, Vol 54, pp. 3777–3782, 2011.

[17] K. Jafar, R. Nazar R, A. Ishak, and I. Pop,"MHD mixed convection stagnation point flow of an upper convected Maxwell fluid on a vertical surface with an induced magnetic field,"*Magnetohydrodynamics*, Vol. 47, pp. 61–78, 2011.